Supporting information

Thermal and UV Light Adaptive Polyurethane Elastomer for Photolithography-Transfer Printing Flexible Circuits

*Jiaxin Shi[1], Zhiqi Wang[1], Tianze Zheng[1], Xueyan Liu[1], Baohua Guo[1], Jun Xu[1]**

[1]Advanced Materials Laboratory of Ministry of Education (MOE), Department of Chemical Engineering, Tsinghua University, Beijing 100084, China

*E-mail: jun-xu@mail.tsinghua.edu.cn

*Tel: +86-10-62784740

Experimental Section

Materials

Polycaprolactone diol (PCL-OH, Alladin, Mn=2000 g mol^{-1}) was dried under vacuum at 110°C prior to use. Isophorone diisocyanate (IPDI, 99%), 4,4-dihydroxybenzophenone (98%), 1,4-diazabicyclo[2.2.2]octane (DABCO, 99%), bis(2,dimethylaminoethyl)ether (BDMAEE, 98%), acrylamide (AM, 99%), 3-(trimethoxysilyl)propyl methacrylate (KH-570, 97%) were purchased from Admas-Beta. Hexamethylene diisocyanate trimer (3HDI, Desmodur N3300) was purchased from Bayer. Dry tetrahydrofuran (THF) and toluene were purchased from Energy Chemical. Ag NWs aqueous dispersion (diameter 30nm, length 100μm, 0.5 wt%) was purchased from Nanjing Xianfeng Science and Technology Co., Ltd. All reagents were used as received except PCL.

Synthesis of the phenol-carbamate containing polyurethane: crosslinked polyurethanes with phenol-carbamate bonds and UV-sensitive units

PU-DHBP-1, PU-DHBP and PU-DHBP-3 were prepared by one-pot process as shown in Scheme 1 and the feeding ratio of different samples is shown in Table 1. In a representative procedure, a charge of 20.00g (10mmol) PCL-OH, 4.45g (20mmol) IPDI, and 0.04g DABCO (0.2 wt% of PCL-OH) solved in 1ml THF was added into a 250ml three-necked flask with a Teflon mechanical agitator, then the temperature was raised to 90°C and held for one hour under stirring. After the prepolymer was synthesized, 3HDI, 4,4-dihydroxybenzophenone and 0.02g BDMAEE (0.1 wt% of PCL-OH) solved in 10ml THF was added into the prepolymer at 90°C and stirred for a few minutes. At last, the bubbles were eliminated under vacuum, then the mixture was poured into a Teflon plate and further cured for 24 hours under dry condition at 60°C. The polymer was further dried under vacuum at 40°C for about 48 h to obtain a light-yellow transparent sheet.

Surface grafting of the PU-DHBP under UV irradiation

Acrylamide aqueous solution (1mol L^{-1}) or KH-570 liquid was evenly dropped on the surface of the PU-DHBP sheet (50μL cm^{-2}), and then a quartz glass was pressed on

the PU-DHBP to form a uniform liquid film. The samples were irradiated with a 200W, 365nm ultraviolet lamp for 30s to initiate polymerization of acrylamide or KH-570. After the grafting was completed, the samples were washed with alcohol and water, then dried under vacuum at room temperature for 24 hours to obtain the final sample.

Self-crosslinking and patterned printing Ag NWs of the PU-DHBP

Cover the PU-DHBP with a light-shielding mask. The samples were irradiated with a 200W, 365nm UV lamp for 10 minutes to fully self-crosslink the irradiated portion. After the irradiation was completed, the mask was removed. Ag NWs were deposed on PTFE membrane by suction filtration (1mg cm^{-2}). The PTFE membrane was covered on the patterned self-crosslinked PU-DHBP, then heated at 100ºC for 30 minutes, and annealed at 50ºC for 12h, so that the Ag NWs adhered to the part covered by the mask.

Self-healing test

In the self-healing test of scratches, the sample with thickness of ca. 1mm was initially put on a glass slide and then scratched by a razor. To observe the self-healing ability of PU-DHBP, the sample was heated at 80 °C for a period and the images under microscope were taken.

In the uniaxial self-healing test, the dumbbell-shaped specimen was cut in half with a razor, then the two pieces were gently brought into contact for 10 s and put into an oven with desiccant to heal under 80ºC without external force. After self-healing, the sample was cooled to room temperature and stored for at least 24h. At last, the healed specimen was tested on tensile tester.

General characterization

Soxhlet extraction was performed in dry THF for 24h in order to calculate the gel fraction. Temperature varying-Fourier transform infrared (FTIR) spectra were collected on a Nicolet 6700 FT-IR spectrophotometer equipped with a deuterated triglycine sulfate detector and a hot stage. Each sample was cast onto a KBr plate to obtain a thin film, on top of which a second KBr plate was placed. The sample sandwiched by KBr plates was put into the hot stage. The transmission spectra were collected with an average of 16 scans for each run at a resolution of 4 cm^{-1} in the range of 4000−500 cm^{-}

^{1} after the sandwiched sample was equilibrated at the desired temperature. Attenuated total reflection infrared (ATR-AR) spectra were collected on a Nicolet 6700 FT-IR spectrophotometer equipped with an ATR accessory. Differential scanning calorimetry (DSC) measurement was conducted on a DSC 250 (TA Instrument) with a heating and cooling rate of 10 °C/min under nitrogen atmosphere. Dynamic mechanical analysis (DMA) was carried out on an DMA Q850 apparatus (TA Instrument) in a tension film mode at temperatures ranging from -80 to 120 °C with a heating rate of 2 °C min^{-1}. The maximum strain was 0.05% and the frequency was 1 Hz. Stress relaxation curves were also obtained using the DMA Q850 in a film clamp mode. Each sample was first equilibrated at a set temperature for 5 minutes, then it was initially stretched to a strain of 5% and the strain was maintained. Dumbbell-shaped specimens for tensile tests were cut from cast sheets using a standard bench-top die according to GB/T-528 (ca. 1mm(thickness) × 2mm(width) × 35mm(length) and a gauge length of 15 mm). Tensile tests were conducted on a JinJian UTM-1432 tensile tester equipped with a 500 N load cell at 25ºC with a 100 mm min^{-1} tensile rate. To evaluate reprocessability, the materials were reprocessed on a lab hot press at 80ºC under 15 MPa for 20 minutes under vacuum. After remolded, the samples were annealed at 50ºC for 24 h in an oven with desiccant to fully equilibrate the reaction of phenol-carbamate. Energy dispersive spectra (EDS) and scanning electron microscope (SEM) photographs were collected on a JEOL 7900F.

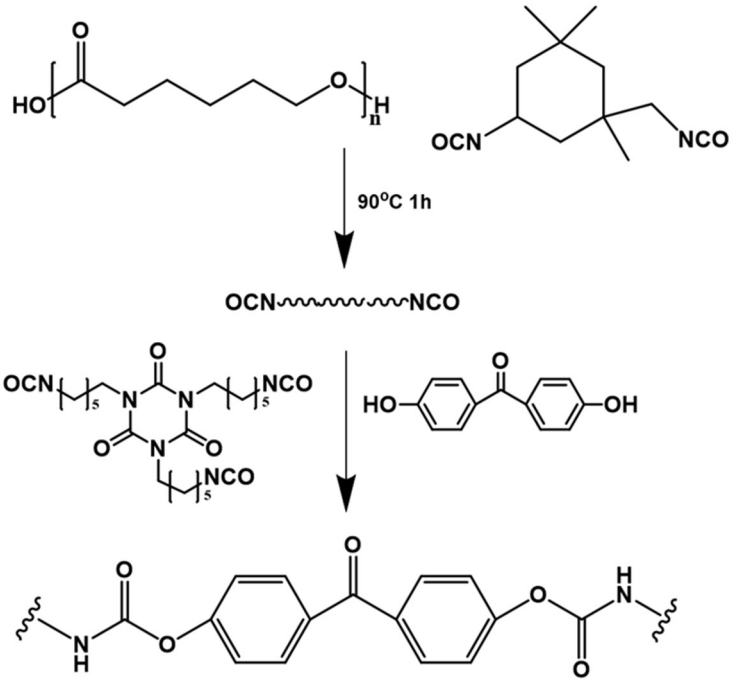

Scheme S1. Synthesis of PU-DHBP samples with covalent adaptable networks and photo-initiator units.

Table S1. Properties of different PU-DHBP samples

Samples	Molar ratio[a])	Young's Modulus [MPa]	Tensile Stress [MPa]	Elongation at break [%]	Toughness [MJ m^{-3}]	T_g [°C]
PU-DHBP-1	1 : 2 : 2 : 2/3	3.7±0.3	12.9±0.7	580±21	28.5±1.9	-3.5
PU-DHBP	2 : 4 : 3 : 2/3	2.8±0.2	21.1±1.8	1055±39	54.7±4.2	-6.3
PU-DHBP-3	3 : 6 : 4 : 2/3	1.5±0.3	11.5±0.9	1270±48	33.7±3.5	-7.6

[a]) The molar ratio of PCL diol : IPDI : 4,4-dihydroxybenzophenone : 3HDI.

Table S2 Swelling and Soxhlet extraction results of the PU-DHBP samples

Sample	Original mass [g]	Mass after swelling test [g]	Gel fraction [%]
PU-DHBP-1	2.045	2.003	97.9
PU-DHBP	1.985	1.911	96.3
PU-DHBP -3	2.088	1.965	94.1

There is a tendency for phase separation of the soft and hard segments of polyurethane, so the monomers need to be carefully selected to avoid incomplete or failure of polymerization due to low miscibility. The commonly used polyols such as polypropylene glycol and poly(tetramethylene ether glycol) are not miscible with 4,4'-dihydroxybenzophenone and cannot be used as oligomers to synthesize transparent

polymeric materials. In contrast, polyester diol is miscible with 4,4'-dihydroxybenzophenone, so we chose flexible poly(ε-caprolactone) diol as the polyurethane soft segment. By adjusting the ratio of PCL diol (M_n~2000), 4,4'-dihydroxybenzophenone and isocyanate, three samples with different cross-linking degrees were prepared (Table S1). The swelling test proved the cross-linked structure of the samples (Table S2).

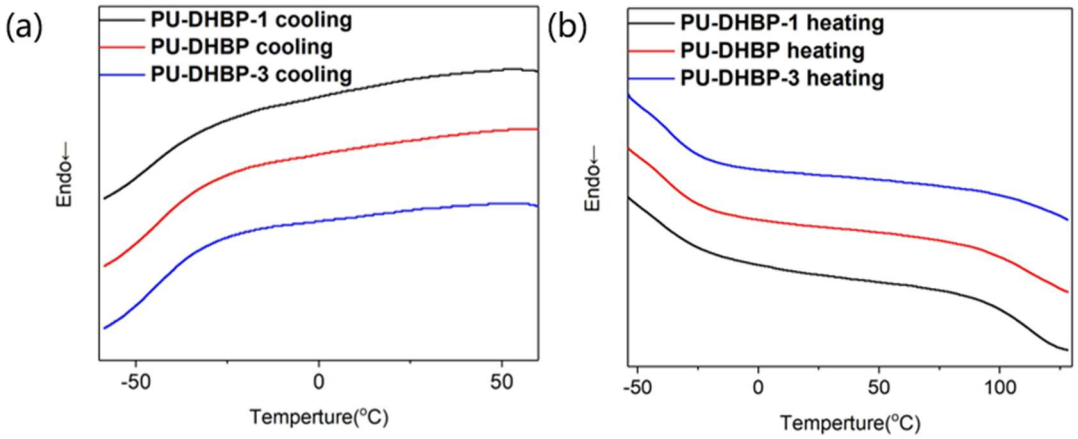

Figure S1. DSC curve of PU-DHBPs after heating to 70°C to eliminate heat history. (a)Cooling process. (b)Secondary heating process.

The only part of PU-DHBP that may crystallize is PCL segment. In Figure S1, except for the glass transition below -25°C and the dynamic bond dissociation endotherm above 70°C, no other signals appeared. Therefore, in PU-DHBPs, the molecular chains are amorphous. Chemical crosslinking and hard segments inhibit the crystallization of PCL.

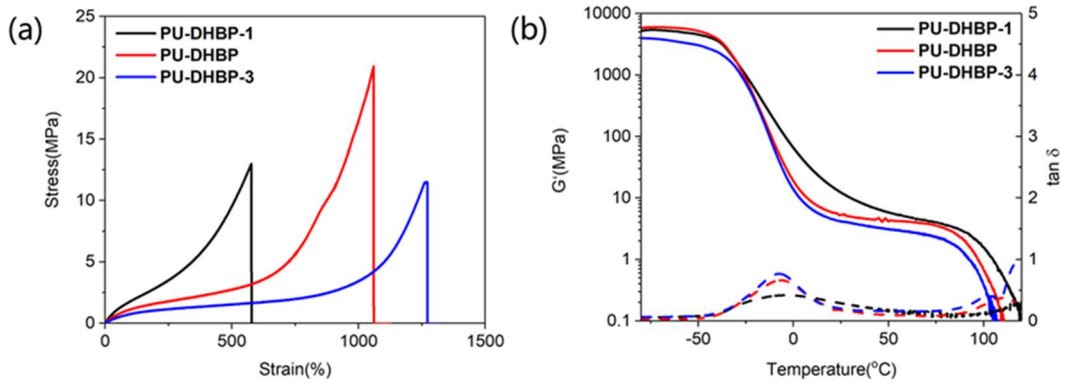

Figure S2. (a)Stress-strain curve of different PU samples. (b)DMA curve of the samples showing storage modulus and dissipation factor tan δ.

Since the molecular chain lengths between the cross-linking points of the three samples are different, the strain at hardening increases with the decrease of the cross-linking degree. During the entire stretching process, hydrogen bonding acts as a dynamic physical interaction and plays the role of energy dissipation. Thus, the low modulus and high strength of PU-DHBP can be attributed to the combined effect of hydrogen bonding and chemical cross-linking.

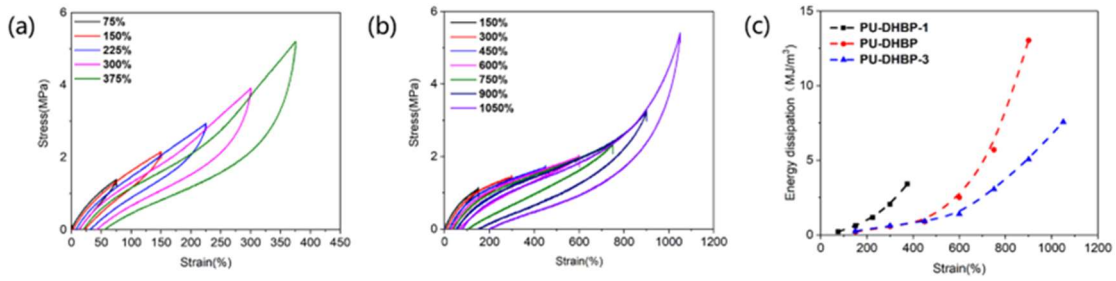

Figure S3. Stress-strain curve of (a) PU-DHBP-1 and (b) PU-DHBP-3 in the cyclic tensile test. (d) Energy dissipation of PUs in the cyclic tensile test at different strain.

In our PUs, the increase of cross-linking degree corresponds to the increase of hard segment content, while the dissipation of polyurethane is largely related to the dissociation of hydrogen bonds in the domain consisted of hard segments[1–3]. Therefore, at the same strain, the amount of energy dissipation increases as the cross-linking degree becomes higher. It should be noted that the residual deformation is controlled by both the hard segment content and the crosslinking degree. Both high content of hard segments and low crosslinking degree results in higher permanent deformation after removal of stress. The energy dissipation of the three samples showed a trend that the greater the maximum strain in each cycle, the faster the dissipation increases. It is precisely because of this mechanism that the low rebound rate of PU-DHBP-1 with high hard segment content and PU-DHBP-3 with low crosslinking degree is caused. Therefore, a proper degree of chemical crosslinking and a moderate content of hard segments are required to meet the low permanent deformation and high repeatability of flexible electronic elastomers.

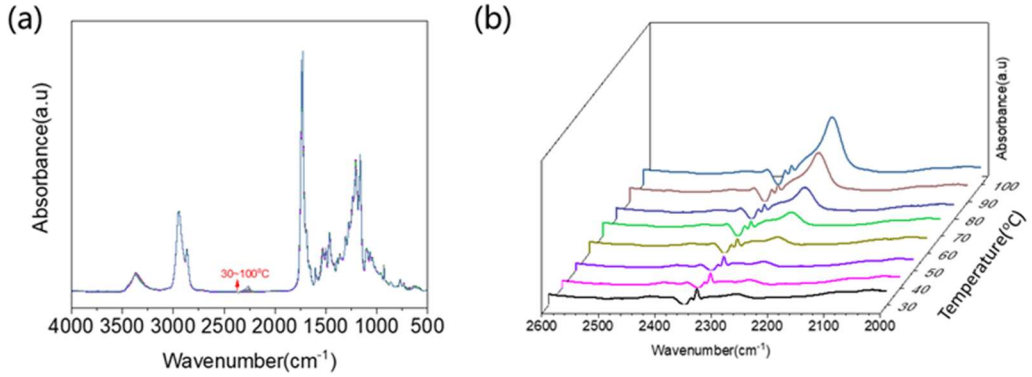

Figure S4. Temperature variable FTIR spectroscopy of PU-DHBP. (a)Overall atlas of 30-100ºC. (b)Change of the free -NCO peak from 30ºC to 100ºC.

Herein, the substituent of bisphenol is a carbonyl group, which has a strong electron withdrawing effect, resulting in a low initial dissociation temperature (~70°C). The dissociation of phenol-carbamate bond is evidenced via the infrared spectra during heating (Figure S4). The free -NCO peak (~2270cm^{-1}) increases gradually with the increase of temperature.

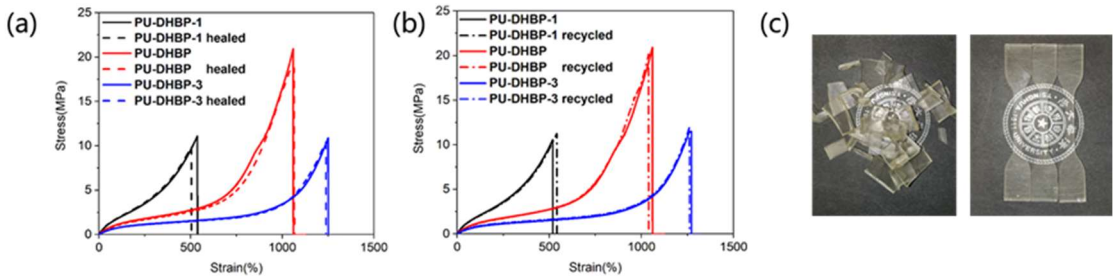

Figure S5. (a) The stress-strain curves of original and the self-healed PUs. (b) The stress-strain curves of original and the reprocessed PUs. (c) Macrophotographs of PU-DHBP before and after reprocessing.

The preparation of polymers into flexible electronic devices has certain requirements on shape and precision, which means that polymeric materials produced in batches need to be remolded. The samples were cut into pieces and hot pressed at 100°C for 20 minutes. All samples could be reprocessed almost perfectly. The tensile test shows that the stress-strain curves of the three samples are very similar before and after reprocessing, indicating good re-processability

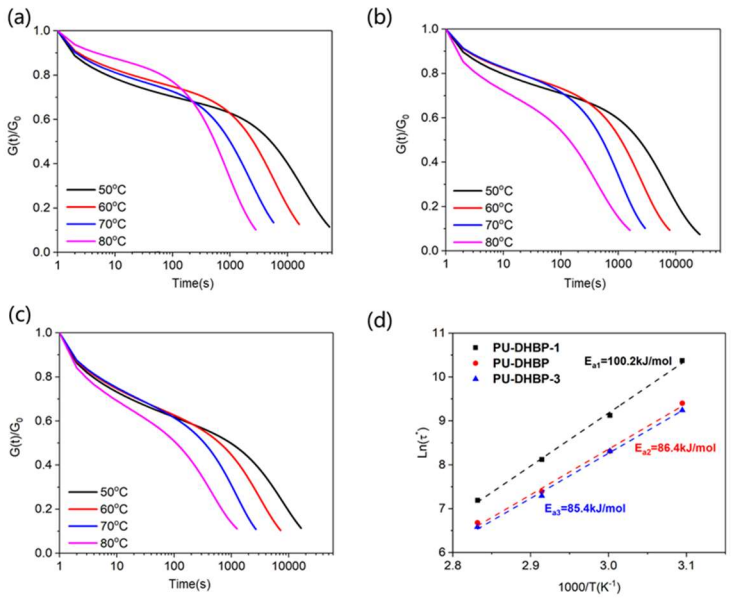

Figure S6. Stress relaxation analysis of (a) PU-DHBP-1, (b) PU-DHBP and (c)PU-DHBP-3. (d) Arrhenius analysis of ln(τ*) versus 1000/T. τ* is the relaxation time determined from the Maxwell fitting of the second segment of the relaxation curve.

As shown in Figure S6, the relaxation curves of the three samples at all test temperatures can be divided into two stages. The first stage is the rapid decline of the modulus within the first tens of seconds, which is related to the rotation of the molecular chain and the dissociation of hydrogen bonds[4]. This stage does not reflect the network rearrangement induced by dynamic covalent bonds. The second stage in which the logarithm of $G(t)/G_0$ has a linear relationship with time, corresponds to the network rearrangement caused by the dissociation of dynamic covalent bonds. In fact, the relaxation in the second stage agrees with the single Maxwell relaxation model. This phenomenon is widespread in dynamic covalent networks and has been analyzed by researchers from the perspective of theory and experiment[5–8]. Therefore, the Maxwell model can be used to fit the second stage of the relaxation curve to obtain the relaxation time of this stage.

When only considering the stress relaxation caused by dynamic covalent bonds, the relaxation time corresponds to the lifetime of the "typical cluster" (the entire network in the gel state), which is positively correlated with the bond lifetime and negatively correlated with the cross-linking degree[6,7]. In this way, the difference in network

rearrangement kinetics of different PU samples is easy to understand. In previous study, it was found that the bond lifetime and relaxation activation energy of IPDI-based phenol-carbamate were significantly lower than that of HDI-based phenol-carbamate[9]. The IPDI/HDI molar ratio in the three samples is in the order: PU-DHBP-3>PU-DHBP>PU-DHBP-1, so as one of the influencing factors, the relaxation time at the same temperature and relaxation activation energy sequence are PU-DHBP-3<PU-DHBP<PU-DHBP-1. In addition, the order in the degree of chemical crosslinking is PU-DHBP-3<PU-DHBP<PU-DHBP-1, which further leads to the trend of relaxation time. The decrease in the cross-linking degree causes the conversion ratio of phenolic group to get closer and closer to the gel point, so the relaxation activation energy is getting closer to the phenol-carbamate dissociation activation energy[6], showing a downward trend. Therefore, in our polyurethane system, the two factors, bond lifetime and cross-linking degree lead together to the difference in the network rearrangement kinetics of the three samples. The larger activation energy in PU-DHBP-1 should be attributed to both the dissociation of dynamic phenol-carbamate bond and the constraining effect of the fixed chemical crosslinking. It should be noted that the chemical relaxation times of PU-DHBP and PU-DHBP-3 with different degrees of chemical cross-linking are not significantly different, implying that the relaxation only results from the dissociation of dynamic bond in the two samples. The similar relaxation time in PU-DHBP and PU-DHBP-3 indicates the same rate constant of bond dissociation in the two samples, which does not vary with the concentration of dynamic bonds. This basic assumption is the theorical basis of the single Maxwell model.

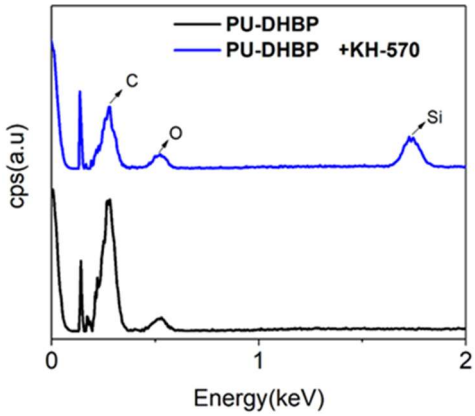

Figure S7. Elemental analysis spectra of ungrafted and grafted KH-570 on PU-DHBP.

The PU-DHBP grafted with KH-570 was subjected to hydrolysis-drying treatment after being irradiated with UV, and a Si-O-Si network was formed on the surface. Surface elemental analysis demonstrates the successful grafting of silicon-containing molecules.

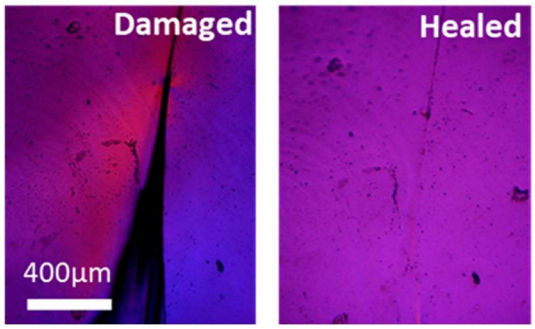

Figure S8. Self-healing micrograph of PU-DHBP after grafting acrylamide at 80°C.

Figure S8 shows that the grafted sample can still achieve obvious self-healing after deep scratching. In fact, the UV irradiation time is short and does not cause a lot of irreversible crosslinking. The amount of polymer grafted on the surface of PU-DHBP is very low (there is almost no obvious weight change in the sample), the UV-sensitive group on the surface and the dynamic covalent bonds in bulk are relatively independent.

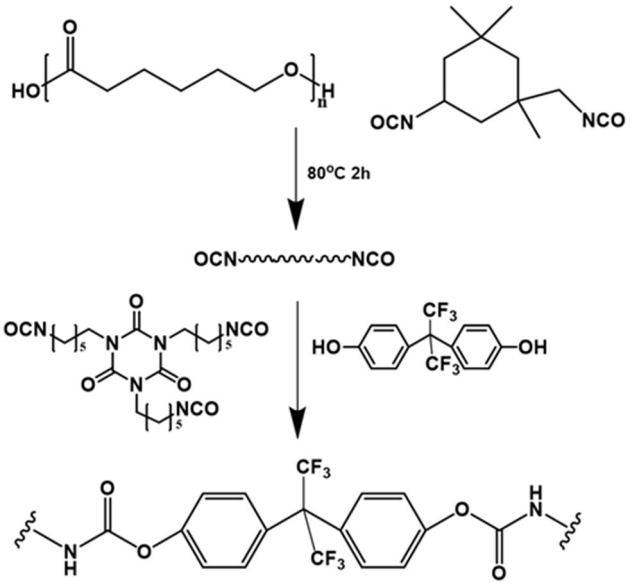

Scheme S2. Synthesis of PU-AF samples with covalent adaptable networks but without photo-initiator units.

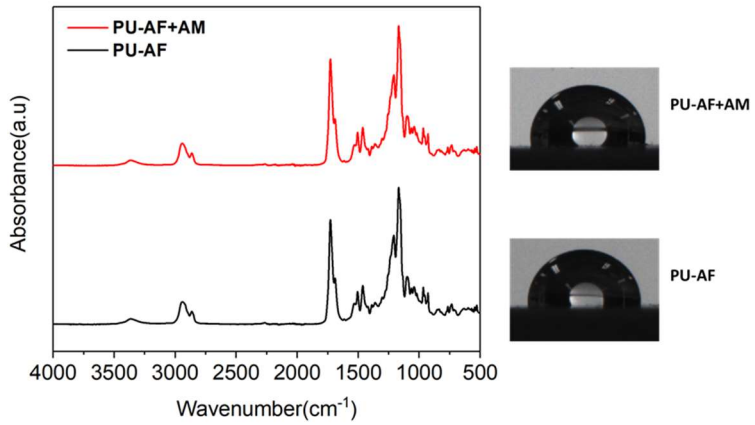

Figure S9. ATR-IR spectra and water contact angle image of PU-AF. The unchanged contact angle indicates no surface grafting after UV irradiation.

In order to prove that the surface grafting is indeed initiated by the benzophenone unit, the control sample PU-AF (Scheme S2) was prepared with bisphenol AF instead of dihydroxybenzophenone. Under the same processing conditions, there is no change in the ATR-IR spectra and water contact angle of PU-AF (Figure S9), which means that PU-AF cannot be grafted on surface, proving the effectiveness of the benzophenone unit.

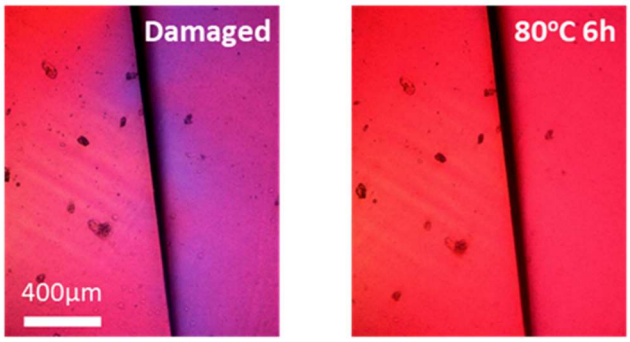

Figure S10. The failed self-healing micrograph of PU-DHBP after 10 min UV irradiation.

The self-healing test was performed on the samples irradiated for 10 minutes, and the scratches hardly had any shrinking trend (Figure S10), which reflected the disappearance of self-healing ability, an inevitable result of irreversible crosslinking.

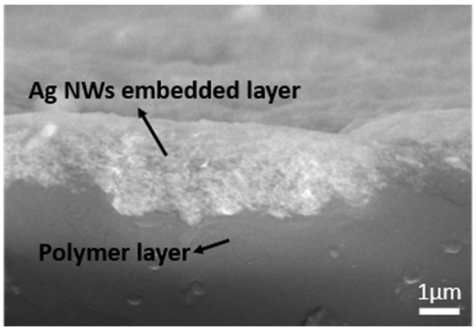

Figure S11. SEM photograph on cross-section of PU-DHBP adhered to Ag NWs at 100ºC for 1h.

The PU-DHBP embedded with Ag NWs was frozen in liquid nitrogen and cut. The Ag NWs-polymer composite layer on the surface and the polymer layer inside were clearly visible at the cross section (Figure S11).

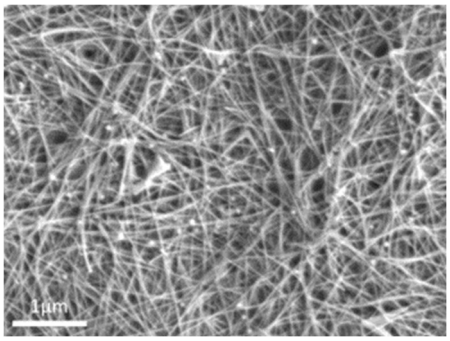

Figure S12. SEM photograph of PU-DHBP adhered with Ag NWs at 80ºC for 1h.

Heated at 80ºC for 1 hour could not obtain an embedded conductive network, and Ag NWs could only be simply stacked on the surface of the polymer (Figure S12). The reason for this phenomenon is that the network rearrangement is slow at 80°C.

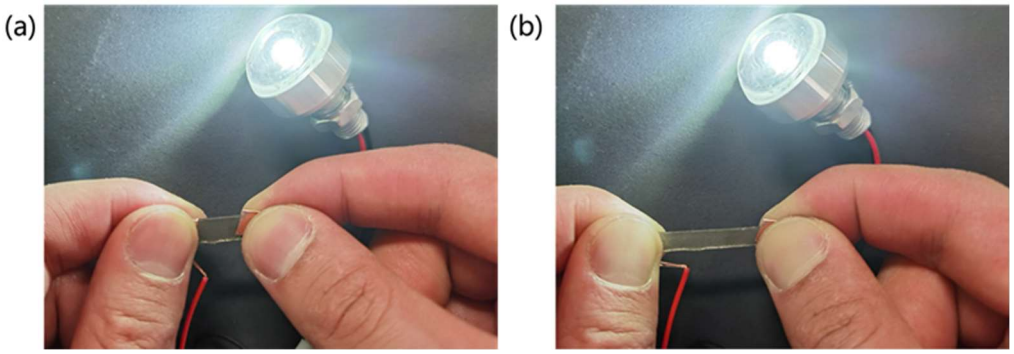

Figure S13. (a) Unstretched and (b) stretched PU-DHBP embedded with Ag NWs as a conductor to light the bulb.

The resistance of the stretchable conductor before and after deformation is stable, so that the brightness of the LED does not change significantly (Figure S13 and S14).

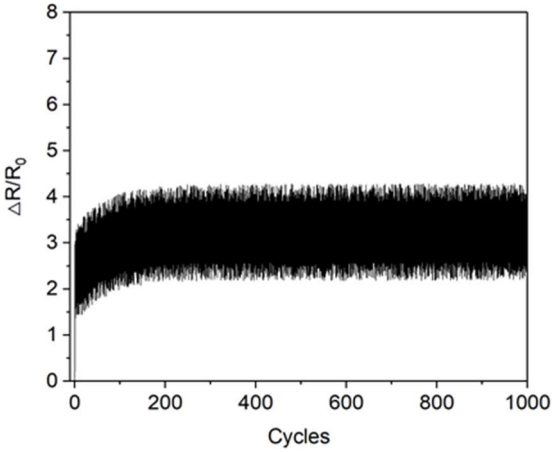

Figure S14. △R/R$_0$ curve due to 50% stretching cycle of PU-DHBP embedded with Ag NWs. The sample is a 20mm×7mm×1.5mm PU-DHBP embedded with Ag NWs.

Since the long-time UV-irradiated region of surface loses its dynamic nature, Ag NWs cannot be firmly adhered to the surface even under heating (Figure S15a). However, the masked regions without UV exposure still retain the characteristics of dynamic covalent cross-linking. After heat treatment, the covalent dynamic network dissociates, so the polymer can be firmly combined with Ag NWs (Figure S15b).

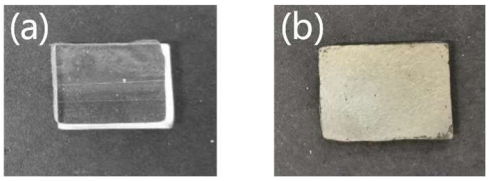

Figure S15. The results of transfer-printing of Ag NWs at 100°C for 1 hour. (a) Ag NWs could not be adhered to the PU with permanently crosslinked surface so the substrate is still transparent. (b) Ag NWs adhered on the PU with dynamically crosslinked surface so the surface is opaque due to existence of Ag NWs.

To demonstrate the possible accuracy with the masked transfer-printing approach, we performed a simple evaluation using a 360-mesh screen as a mask. The mesh-like structure was largely preserved after fabrication (Figure S16), proving that this process can reach a precision of tens of microns.

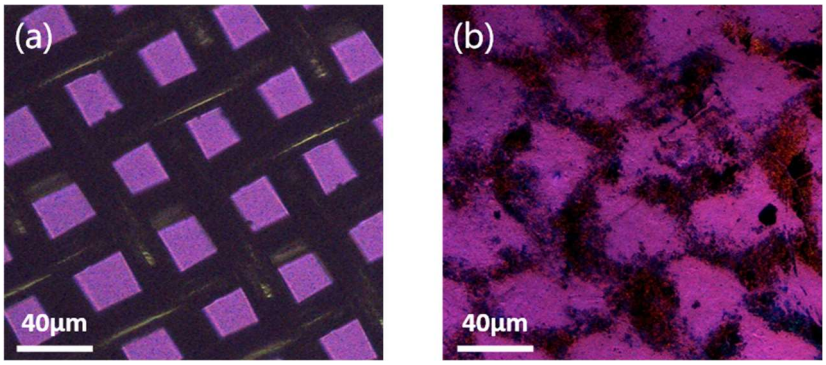

Figure S16. Microscope photographs of (a) 360-mesh screen and (b) Printing Ag NWs on PU-DHBP with 360-mesh screen as mask.

To demonstrate the versatility of the photolithography-transfer printing strategy, we printed multi-walled carbon nanotubes onto the UV exposed half of a rectangular PU-DHBP sample and demonstrated the conductivity of printed circuit by lighting up a LED (Figure S17). Multi-walled carbon nanotubes are less conductive than silver nanowires, so the embedded multi-walled carbon nanotubes can only make the LED weakly emit light.

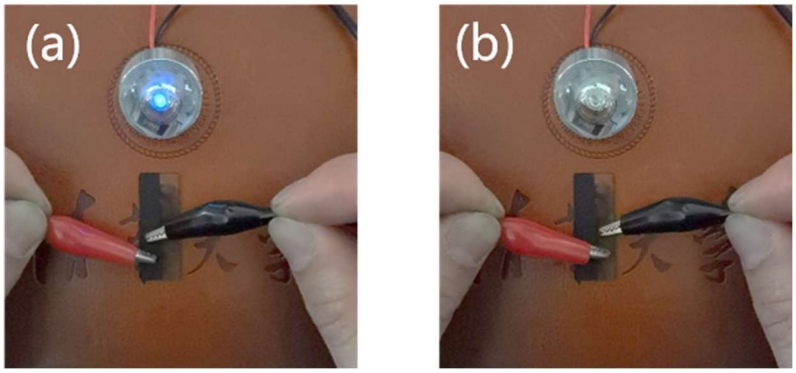

Figure S17. Printing multi-walled carbon nanotubes onto half-area-UV exposed rectangular PU-DHBP. (a) The left black half with transfer printed carbon nanotubes is conductive. (b) The right transparent self-crosslinked half without carbon nanotubes is non-conductive.

Compared to other fabrication methods for patterned flexible circuits, UV self-crosslinking offers an additional advantage. The self-crosslinked layer can form a protective skin layer on the dynamic covalent polymer surface. Dynamic covalent polymers are prone to slight deformations, especially at sharp edges, due to their slow flow when processed at high temperatures. In addition, it is also easy to generate bubbles at the overheated substrate. After UV self-crosslinking treatment, the irradiated

part can provide support and maintain the stability of the shape of the designed product (Figure S18).

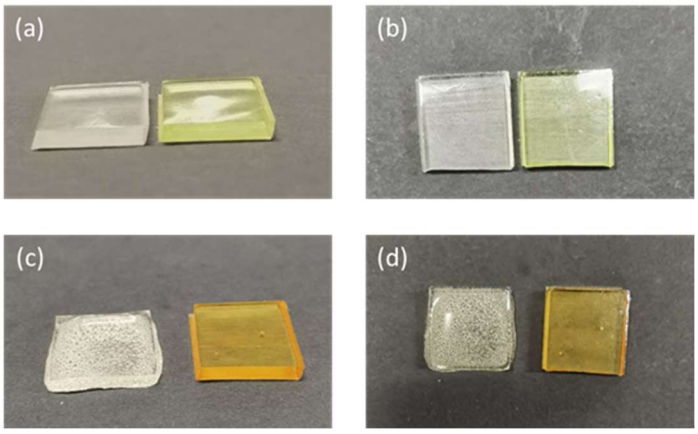

Figure S18. Photographs of (a-b) pristine PU-DHBP (left) and UV irradiated PU-DHBP (right), (c-d) pristine PU-DHBP (left) and UV irradiated PU-DHBP (right) heated at 120°C for an hour.

Reference

[1] T. Zheng, Y. Zhang, J. Shi, J. Xu, B. Guo, *Mol. Simul.* **2021**, *47*, 1258.

[2] T. Li, C. Zhang, Z. Xie, J. Xu, B. H. Guo, *Polymer.* **2018**, *145*, 261.

[3] T. Zheng, T. Li, J. Shi, T. Wu, Z. Zhuang, J. Xu, B. Guo, *Macromolecules* **2022**, *55*, 3020.

[4] L. H. Sperling, *Introduction to Physical Polymer Science: Fourth Edition*, **2005**.

[5] X. Kuang, G. Liu, X. Dong, D. Wang, *Mater. Chem. Front.* **2017**, *1*, 111.

[6] A. N. Semenov, M. Rubinstein, *Macromolecules* **1998**, *31*, 1373.

[7] A. N. Semenov, M. Rubinstein, *Macromolecules* **1998**, *31*, 1373.

[8] G. A. Parada, X. Zhao, *Soft Matter* **2018**, *14*, 5186.

[9] J. Shi, T. Zheng, Y. Zhang, B. Guo, J. Xu, *Polym. Chem.* **2021**, *12*, 2421.